The use of remote sensing data to improve the modelling of skin temperature

Isabel F. Trigo

Instituto de Meteorologia
Rua C-Aeroporto, 1700 -077 Lisboa, Portugal
Isabel.Trigo@meteo.pt

Abstract

The assessment of ECMWF land surface temperature presented here is based on the intercomparison of modelled and observed clear sky radiances of Meteosat window channel. The study is carried out for two periods covering distinct seasons, for Meteosat-7 disk. Such comparison enabled the detection of gross errors in the observations, mainly associated with the cloud screening, and the evaluation of the model's performance. Results show an underestimation of the diurnal cycle of model brightness temperature in clear-sky conditions, particularly over arid and semi-arid regions, which reflect a corresponding misrepresentation of the daily amplitudes of model skin temperature.

Sensitivity experiments suggest model deficiencies are likely to be linked to inadequate values of surface parameters directly associated with the surface-to-atmosphere coupling, particularly the roughness lengths for momentum and for heat. Finally, some preliminary results of adjustments to the land surface scheme, that might improve the ECMWF model representation of skin temperature, are also presented here.

1. Introduction

The surface parameterization scheme introduced in a numerical weather prediction (NWP) model plays a crucial role in the representation of the boundary layer forcing. The quality of surface and lower troposphere forecasts (e.g., near surface temperature, humidity, cloudiness), and of the reproduction of soil variables depends to a large extent on the modelled surface-atmosphere interactions. Also the increased usage of remote sensing information for assimilation in NWP models requires a good quality model background of the quantities to be assimilated. In particular, the remote sensing channels that peak in the lower troposphere need a good a priori knowledge of surface or skin temperature, a requirement which is still far from being reached over land.

The European Centre for Medium-Range Weather Forecasts (ECMWF) land surface parameterisation scheme, TESSEL (Tiled ECMWF Scheme for Surface Exchanges over Land; van den Hurk et al 2000), has up to six independent fractions (tiles) for every land grid box, with separate skin temperatures and fluxes. Each tile has its own characteristics defining separate heat and water fluxes used in an energy balance equation solved for the tile skin temperature.

The evaluation of such land surface schemes is a complex problem. Traditionally this has been done using data from field experiments (e.g. Betts et al. 1996), despite the strong limitations associated with data availability. Satellite-derived data has been increasingly used for validation purposes (e.g. Rhoads et al 2001), as it allows the assessment of the models' performance over large areas and for long periods of time. Recently, Trigo and Viterbo (2003; hereafter TV03) have compared Meteosat clear sky radiances in the window channel (10.5 – 12.5 μm) with their ECMWF model equivalent. The results obtained by TV03, which constitute the main motivation for the present work, allowed for the identification of systematic errors in the observational data and the assessment of the model's performance. The former are mostly associated to the cloud processing for Meteosat imagery, performed at EUMETSAT, and can be at least partially overcome by using a further stricter criterion for the elimination of clouds. It was also found that, under clear

sky conditions, the modelled diurnal cycle of window channel brightness temperatures, and thus of land surface temperature, tends to be greatly underestimated, particularly over arid and semi-arid regions. A brief description of these results will be presented in section 2.

In order to identify the main causes for the poor representation of land surface temperature by the model, a set of sensitivity experiments is performed using a simplified version of the ECMWF model – the single column model. The results obtained, discussed in section 3, point towards deficiencies in the surface-atmosphere aerodynamic coupling over land. Finally, the use of remote sensing data to upgrade and test land surface parameterisation schemes is explored in section 4. The results are analysed within possible frameworks for surface fluxes modelling.

2. Meteosat and ECMWF brightness temperatures in the 11μm channel

Meteosat-7 window channel radiances (10.5 – 12.5 μm band) were compared with their ECMWF model equivalent. The measurements of top of atmosphere (TOA) brightness temperatures, hereafter Tb_obs, were previously pre-processed at EUMETSAT to eliminate cloudy pixels. The so-called clear sky radiances (CSR) (van de Berg et al. 1995) are obtained by averaging the values diagnosed as "clear sky" within areas of 16 by 16 pixels. However, one must be aware that such Tb_obs values may still be contaminated by a significant amount of cloudy pixels (TV03).

The modelled brightness temperatures are obtained from ECMWF background fields presented to the data 4D-Var assimilation scheme (Rabier et al. 2000). Although Meteosat 11 μm radiances are not assimilated at ECMWF, 3-hourly background brightness temperatures for the window channel (Tb_bg) are obtained using the background profiles of temperature and humidity, and the skin temperature as input to the Radiative Transfer for TOVS model version 5 (RTTOV-5) (Eyre 1991; Saunders et al. 1999). The RTTOV-5 model ignores the model cloud cover, liquid and ice water, and thus the Tb_bg provided are always considered clear sky.

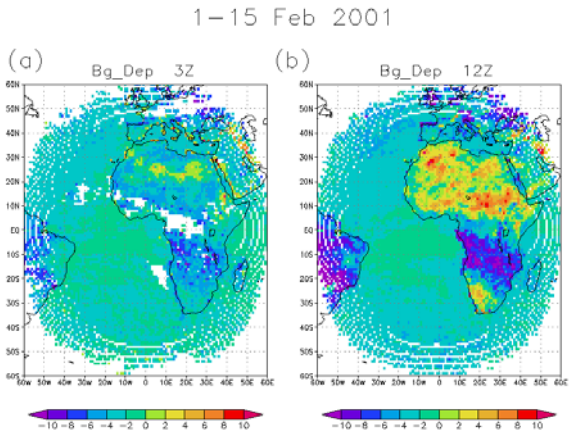

Figure 1: "Tb_obs – Tb_bg" (K) averaged for the period 1-15 February 2001 obtained for Meteosat-7 at (a) 3 UTC and (b) 12 UTC.

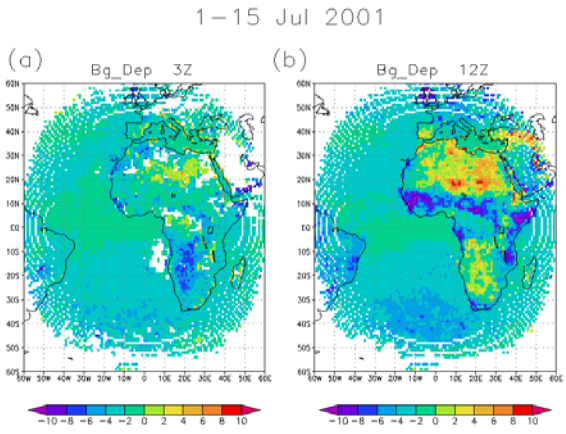

Figure 2: As in Fig.1, but for the period 1-15 July 2001.

The corresponding regions with strong daytime negative bias for February 2001 are mainly constrained to the 0° – 20°S latitudinal band (Fig. 1b). For the next months the daytime negative values of such brightness temperature departures, mainly between 10°S and 20°S, weaken and are replaced by a positive bias over southern Africa in July (Fig. 2b). Meanwhile, the negative bias band has moved northwards following the intertropical convergence zone (ITCZ), linking the main factors guiding the spatial distribution of the most pronounced negative/positive Tb difference patches in the subtropics to the local rainy/dry season. As further

discussed below, these may be related either to the observations, such as deficiencies in the cloud clearing, or to the model, e.g., the inadequacy of climatologically fixed model parameters, such as albedo, vegetation cover and type, or model variables, such as soil moisture, humidity profiles / total water vapour content.

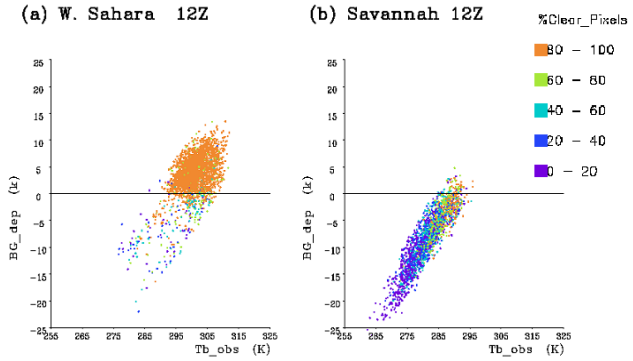

Figure 3 - Scatterplots of the "Tb_obs – Tb_bg" (BG_dep in K) against Tb_obs (K), for (a) Western Sahara, and (b) Savannah at 12 UTC. The points are coloured according to the percent of clear sky pixels taken into account for each observation.

The percent of clear sky pixels corresponding to each observation (hereafter %_ClearSky) appears to be strongly associated with the occurrence of negative or positive values of "Tb_obs – Tb_bg". Figure 3 shows scatterplots of "Tb_obs – Tb_bg" versus Tb_obs obtained for the period 1-15 February 2001, and for two limited areas within Meteosar-7 disk, namely the Western Sahara (0°E - 10°E; 20°N - 30°N), and Savannah (22°E - 32°E; 18°S - 8°S) dominated by underestimation and overestimation of the diurnal cycle of brightness temperatures, respectively; the points are coloured according to the %_ClearSky. In the case of the Sahara (Fig. 3a), the two tails of negative "Tb_obs – Tb_bg" values correspond mostly to observations with low %_ClearSky, while positive differences are associated with high values of %_ClearSky. A similar pattern is followed for the Savannah limited area (Fig.3b), which is under the influence of the ITCZ during the February 15-day period. There, cases with values of the %_ClearSky over 80%, and with positive "Tb_obs – Tb_bg" are almost non-existent. It is suggested that the %_ClearSky may be considered as an indicator of the probability of Tb_obs not being contaminated by cloudy pixels (see TV03 for further details). Thus a further cloud screening of the observations, using a minimum threshold (e.g., 80% or 90%) for the %_ClearSky, should be performed before using the observed brightness temperatures.

Over arid and semi-arid (clear sky regions), such as the Western Sahara limited area, the atmosphere is fairly transparent for the window channel. Consequently, the discrepancies between the modelled and observed brightness temperatures to a large extent reflect how well the skin temperature is simulated by the ECMWF model. Furthermore, the diurnal variations of "Tb_obs – Tb_bg" give a good indication of how the diurnal cycle of the surface temperature is being reproduced, since adjustments of surface emissivity have very little effect on the daily amplitude of TOA brightness temperatures. The next step is to identify the main reasons for the underestimation of land surface temperature by the ECMWF model.

3. Sensitivity Experiments

A set of experiments has been carried out using the ECMWF single column model (SCM; Köhler and Teixeira, 2002). Their aim is the identification of the surface variables and/or parameters, which are more directly involved in the underestimation of the diurnal cycle of land surface temperature, particularly in arid and semi-arid regions.

The sensitivity experiments, conducted for 24-hour periods, explore "poor man's parameter estimation", i.e., each surface parameter, from a pre-defined set, is changed at the time to study its impact on the modelled TOA brightness temperature. Similarly, the influence of model surface variables is studied by varying the initial conditions for the 24-hour periods of each variable. The parameters and variables taken into considerations, as well as their impact on the modelled diurnal cycle of brightness temperature are summarised in Table 1.

Surface Variable/Parameter	**Impact on Tb Amplitude**
Albedo	Negligible
Emissivity	Negligible
Skin Layer Conductivity	Negligible
Roughness Length for Momentum	Small/Moderate
Roughness Length for Heat	Moderate/High
Soil Moisture	Moderate/High
Soil Temperature	Negligible

Table 1: Sensitivity of the amplitude of modelled brightness temperatures to surface variables and surface parameters, based on experiments performed using the ECMWF SCM.

Although emissivity is an important parameter for the modelled TOA brightness temperatures, its impact on the modelled diurnal cycle is very small. Figure 3 shows the SCM brightness temperature obtained for one site in the Western Sahara (8.25°E, 26.87°N), for the 3rd February 2001. Over that site the ECMWF full model underestimates the daily amplitude of Tb_obs by over 7K. The SCM was run using emissivity values of 0.93 -typical value expected for very dry regions, such as the chosen site-, 0.96 -control run-, and 0.99 -characteristic of very moist surfaces and thus unrealistic for the arid surface of the site. The results show that the mean difference between the lower (0.93) and higher (0.99 emissivity) curve of brightness temperature is about 3K, while the difference between the amplitude of the same two curves, is of the order of 0.7K.

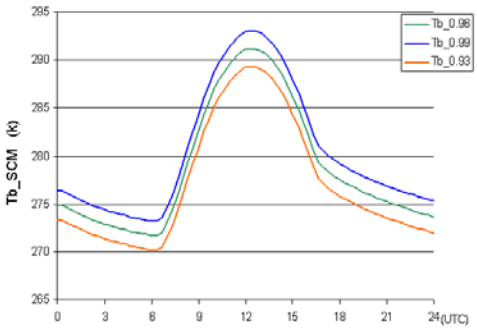

Figure 4 – SCM TOA brightness temperatures (K) obtained for a site in the Western Sahara (8.25°E, 26.87°N), for the 3rd February 2001, using three different emissivity values: 0.93, 0.96 (the control run), and 0.99.

The sensitivity experiments of modelled brightness temperatures to surface emissivity confirm that the underestimation of the amplitude of Tb_obs by the ECMWF described in the previous section may only be accounted for by a corresponding underestimation of the modelled surface or skin temperature. As might be expected, the parameters that had the largest impact on the amplitude of Tb, roughness length for heat, and to a lesser extent roughness length for momentum, are directly associated with the model representation of

turbulent transfer of heat (and momentum) between the surface and the lowest model level. As shown in Fig. 4, decreasing the roughness length for heat (Z_{oH}) by a factor of 100, produces an increase of the amplitude of the modelled brightness temperatures by 2K, with little impact on other modelled variables such as 2m temperature, or 2m dew point.

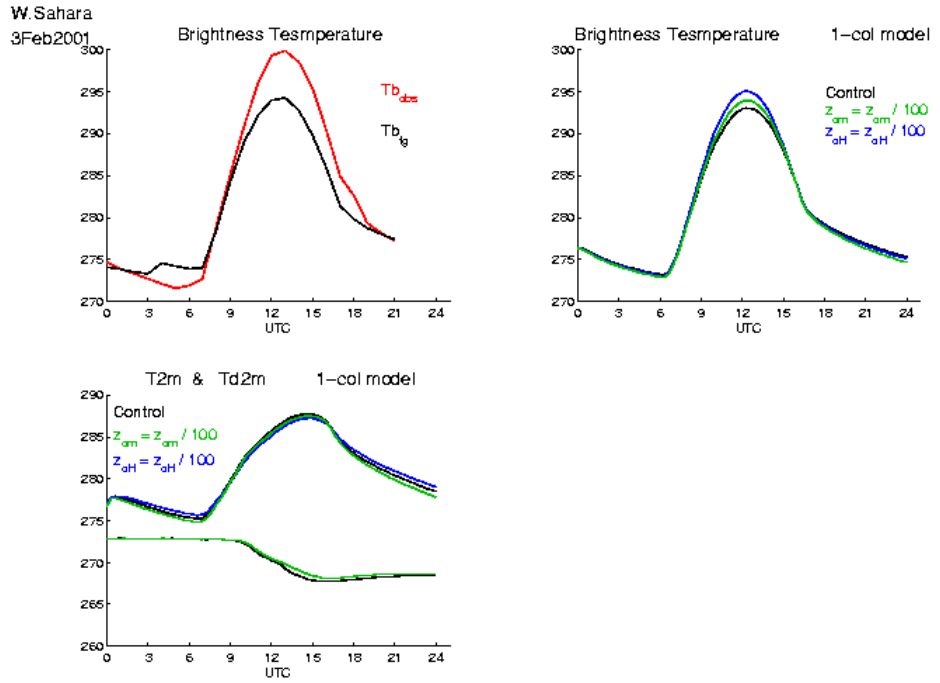

Figure 5 – Daily cycle of the observed (Tb_{obs}; top left) and the full ECMWF model (Tb_{fg}; top left) brightness temperatures (K) for a site in the Western Sahara (8.25°E, 26.87°N), on the 3rd February 2001. The remaining panels show the SCM brightness temperatures (top right), and 2m temperature and 2m dew point (bottom left), obtained with the SCM control run (black), and when the roughness length for momentum (Z_{om}) and for heat (Z_{oH}) are reduced by a factor of 100, respectively.

4. A revised land surface scheme

The use of satellite information to adjust and test model surface parameterizations has great potential over measurements obtained from field experiments (e.g. Betts and Beljaars, 1993; Malhi, 1996), particularly since experiments could be easily performed over wide regions (such as the Meteosat disk). This section presents the results obtained with a two-source approach for the estimation of bare soil and vegetation energy fluxes (Norman et al., 1995; Kustas and Norman, 2000).

For dry, snow free conditions, the surface sensible heat flux is estimated by TESSEL as a weighted average over three tiles – low vegetation, high vegetation, and bare ground. The aerodynamic resistance (*Ra*), which depends on tile surface parameters (such as roughness lengths) and stability functions, represents the resistance to heat transfer between the tile and the lowest model (Fig. 6a).

Over (partially) vegetated areas, the clumping of vegetation into the two vegetation tiles may affect the wind speed within the canopy layer, and thus the resistance of the surrounding bare soil area, to heat transfer. This could lead to the overestimation of sensible heat fluxes, particularly over semi-arid regions, and thus to the underestimation of diurnal cycles of skin and TOA brightness temperatures. To overcome this problem, a resistance, *Rs*, to the transfer of heat in the surface layer is introduced, as schematically represented in Fig. 6b.

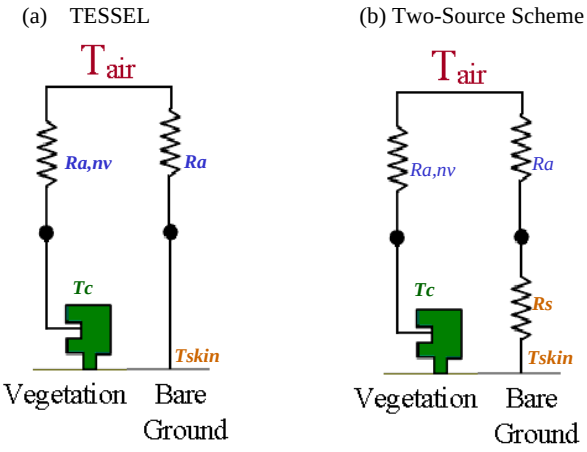

Figure 6 – Schematic resistance representation of the transfer of turbulent sensible heat between the surface and the lowest model level (a) in the current version of TESSEL (control); and (b) in the experimented version, with an extra resistance (Rs) added to bare soil tile.

The extra resistance, *Rs*, to the transfer of heat between the surface and the lowest model level should be applied to bare soil portions within sparsely vegetated areas. For simplicity, the formulation:

$$R_S = \frac{1}{a + b\,u_*^2} \tag{1}$$

where *a* and *b* are fixed parameters (a = 1x10^{-2} ms^{-1}, b= 6x10^{-2} m^{-1}s), and u_* is the friction velocity, is applied to the bare soil tile in the TESSEL scheme. The formulation of *Rs* in (1) was first derived to adjust SCM simulations of Tb amplitudes to Meteosat-7 observations.

Accordingly, sensible heat fluxes over dry, snow free vegetation tiles, and over bare soil tiles are computed, respectively as:

$$H_{nV} = \rho c_p \frac{T_{air} - T_c}{R_{a,nV}} \tag{2}$$

$$H_{bare\_soil} = \rho c_p \frac{T_{air} - T_{skin}}{R_a + R_s} \tag{3}$$

where *nV* denotes low or high vegetation, *Tair* is the temperature of the lowest model level, *Tc* (*Tskin*) is the skin temperature for vegetation (bare soil) tiles, and *Ra*… is the aerodynamic resistance.

The parameters in *Rs*, are obtained as a compromise for the required adjustments to TOA Tb over the whole arid and semi-arid regions within the Meteosat disk. Over the Sahel region, where daytime discrepancies between observed and modelled TOA Tb may reach values of 8 K or more in the dry season, the fraction of bare soil tile is of the order of 0.35. Since the extra resistance in the surface scheme is applied to bare soil tiles only, considerably higher *Rs* values would be necessary to compensate for the relatively small bare soil fractions over those regions, dominated by the "tall grass" vegetation type. To overcome this problem maintaining the dependency of the surface resistance to wind over bare ground only, the roughness length for heat of that vegetation type was decreased by a factor of 100 (Z_{oH} = 10^{-4} m), with respect to the value assigned in the control run (Z_{oH} = 10^{-2} m). It is likely that this roughness parameter should also be revised for other (low) vegetation types, although that was not attempted here.

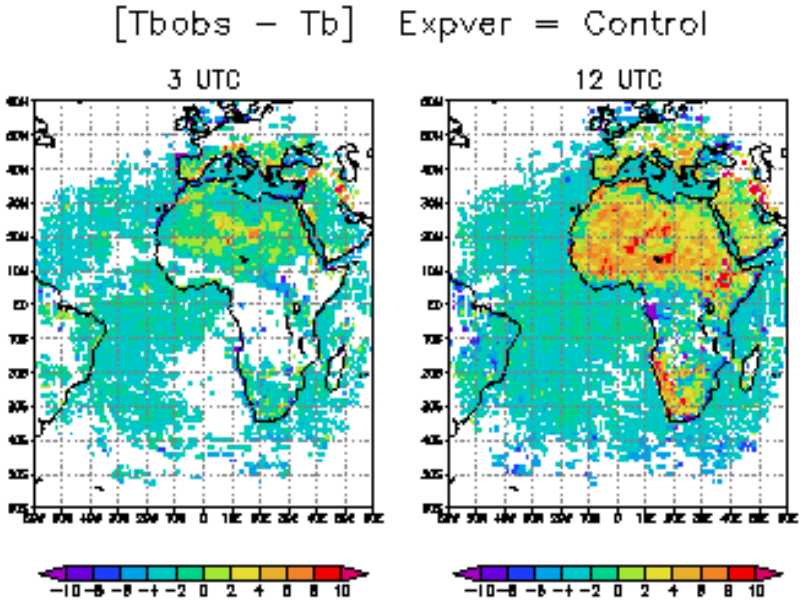

Figure 7: "Tb_obs – Tb_ECMWF" (K) averaged for the period 1-15 February 2002 obtained using the control run at 3 UTC (left) and 12 UTC (right), respectively

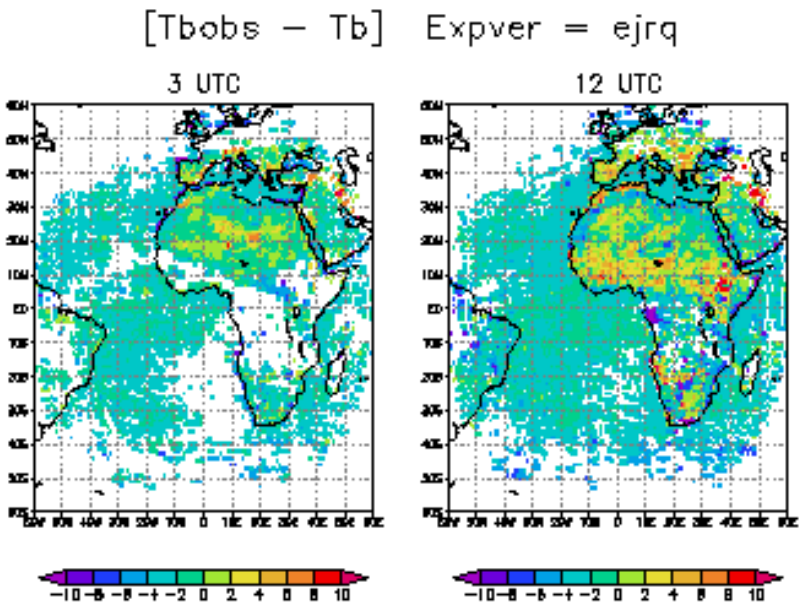

Figure 8: As in Figure 7, but using the extra resistance Rs in TESSEL.

The differences between observed and modelled TOA Tb, averaged for the 1-15 Feb 2002 period, are shown for the control run (Fig. 7), and for the modified TESSEL, with the extra bare soil resistance, *Rs*. The control run was carried out using the so-called 26R3 cycle model version, with a modification to the prescribed roughness length for momentum, Z_{oM}. In the version used here, the Z_{oM} parameter represents the effect of turbulent transport of small-scale surface elements, such as vegetation and surface obstacles, while the effect of subgrid orographic drag is treated separately.

Following the results discussed in section 2, only cases with the percent of clear sky pixels higher than 90% are taken into account. As a result, (semi-)arid regions in Fig. 7 exhibit even higher positive Tb differences than those shown in Fig.1, while the band with negative Tb departures in the subtropics is considerably attenuated.

The new resistance *Rs* for bare soil tiles has little effect on nigh time Tb, leading to very similar 3 UTC fields shown in Figs. 7 and 8. The daytime Tb over (semi-)arid regions are now warmer, which reduces the 12 UTC model bias from 4-to-10K (Fig. 7) to values around –2-to-4K (Fig.8).

The results obtained over two areas, one in the Sahara (5ºE-15ºE; 20ºN-30ºN), dominated by desert and semi-desert tiles, and the other in the Sahel (5ºE-15ºE; 10ºN-20ºN), dominated by tall grass vegetation type, are summarised in Figs. 9 and 10. The diurnal cycles of modelled TOA brightness (Fig. 9), and 2m-temperatures (T2m; Fig. 10) correspond to averaged 3-hourly values over the 1-15 Feb 2002 period and over each area; the observations available for each area are also shown (Meteosat-7 and synoptic stations, respectively). TOA Tb obtained using the modified version of TESSEL follow closely the Meteosat measurements. As expected from the sensitivity experiments performed with the SCM, the impact on T2m is relatively small (of the order of 1K, or less). In this case, the comparison with observed values is particularly difficult, due to the scarce number of synoptic stations available (7 in the Sahara region, and 10 in the Sahel), and to their (non-uniformly) spatial distribution.

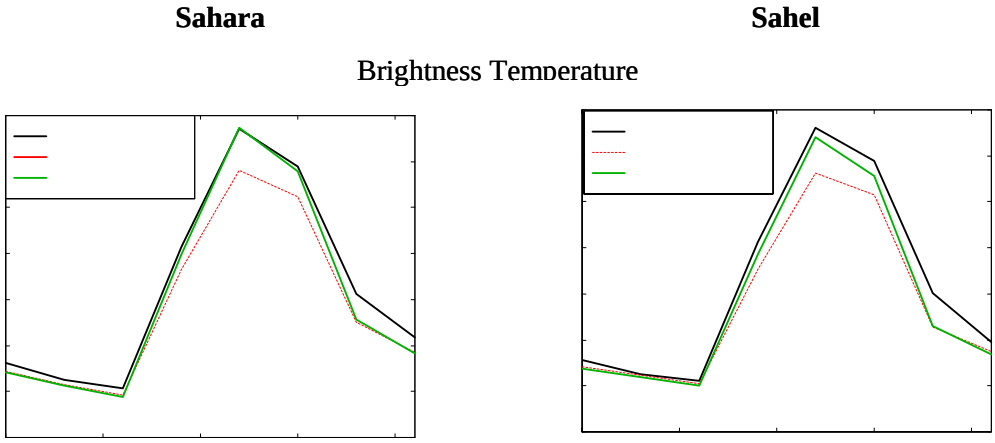

Figure 9: 3-Hourly TOA Tb (ºC) averaged over the 1-15 Feb 2002 period, and over each of the following areas: Sahara (5ºE-15ºE, 20ºN-30º; left panel), Sahel (5ºE-15ºE, 10ºN-20º; right panel).”- -“ – control run; “–” – modified run; “–” – observations (Meteosat-7).

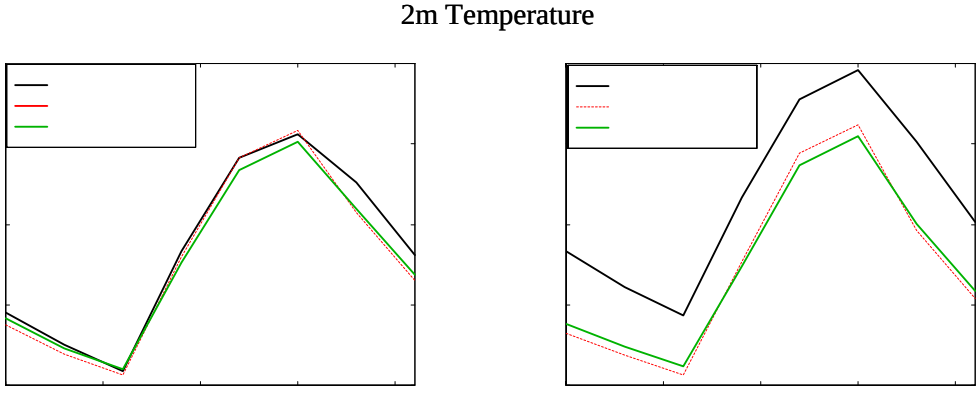

Figure 10: As in Fig.9, but for 2m- temperature (ºC). The observations are obtained from synop stations available within each area.

Ultimately, the new extra resistance, *Rs*, to the transfer of heat between the surface and the lowest model level over bare soil, aims the adjustment of the diurnal cycle of model TOA Tb to the observations. *Rs* allows the wind shielding effect of surrounding vegetation and/or surface obstacles to be taken into account in the

estimation of bare soil sensible heat fluxes (3). Figure 11 shows the behaviour of TOA Tb amplitudes (Tb at 12 UTC minus Tb at 3 UTC) as a function of the wind at the lowest model level (~10m). The Tb amplitudes obtained with the modified version of TESSEL follow well the observations for both studied areas (Fig. 11); the bias of Tb amplitude decreases from 4.3 K (5.4 K) obtained with the control run to –0.5K (1.3K) obtained with the modified TESSEL, for the Sahara (Sahel) region.

5. Conclusions and further work

The comparison between observed and modelled TOA radiances for the 11μm channel suggests the Meteosat-7 clear sky brightness temperatures, produced by EUMETSAT, may still have a significant amount of cloud contaminated pixels. The identification of Meteosat-7 clear sky pixels is particularly difficult for tropical areas under the influence of the ITCZ, where many of the observations are likely to be cloud contaminated. This problem may be solved by performing a further cloud screening to the observations, such as requiring a minimum value of the respective %_ClearSky (e.g. 80% or 90%). The instruments on-board Meteosat Second Generation (MSG), operational since February 2004, have considerably more channels (12) and a higher spatial and temporal resolution, which allow the use of more accurate cloud processing algorithms (Lutz, 1999).

Under clear sky conditions, the diurnal cycle of the window channel brightness temperatures tends to be greatly underestimated by the model, particularly over arid and semi-arid regions (TV03). The sensitivity analysis described in section 3 confirmed that such underestimation is associated to a misrepresentation of the daily amplitudes of the model surface temperature. Although the emissivity values prescribed in the ECMWF model comprise a very limited number of categories, updating the values for a wider variety of land cover types can only reduce the model bias; its impact on the amplitude of the model brightness temperature is very small. Instead the results from the sensitivity experiments point towards inadequate values of surface parameters directly associated with the surface-to-atmosphere coupling, in particular the roughness length for heat (Z_{oH}).

Although not shown, values of Z_{oH} estimated to compensate for the misrepresentation of TOA Tb amplitudes in semi-arid regions, exhibit strong dependency on the wind speed at the lowest model level. It is suggested that such dependency may arise from an overestimation of near surface wind associated with the shielding effect of surface obstacles. This is likely to be particularly pronounced in sparsely vegetated areas, where the vegetation is clumped into the low (or high) vegetation tile, and the bare soil fraction is treated as completely vegetation free. But such wind shielding may still be present in desert areas despite the lack of vegetation, being in that case associated with other surface obstacles.

Following previous studies on the use of a two-source approach for the modelling of sensible heat flux (Norman et al., 1995; Kustas and Norman, 2000), a new resistance, *Rs*, to the turbulent transfer of heat between the surface and the lowest model level is added to the aerodynamic resistance, for the bare soil tile. The *Rs* formulation (1) used here depends on the friction velocity, and on two parameters adjusted using the SCM model. The revised version of TESSEL proved to be efficient in reducing the model bias in the daily amplitudes of brightness temperatures. The modified model produces warmer daytime skin temperatures over most arid and semi-arid regions, although the impact on other model variables is relatively low.

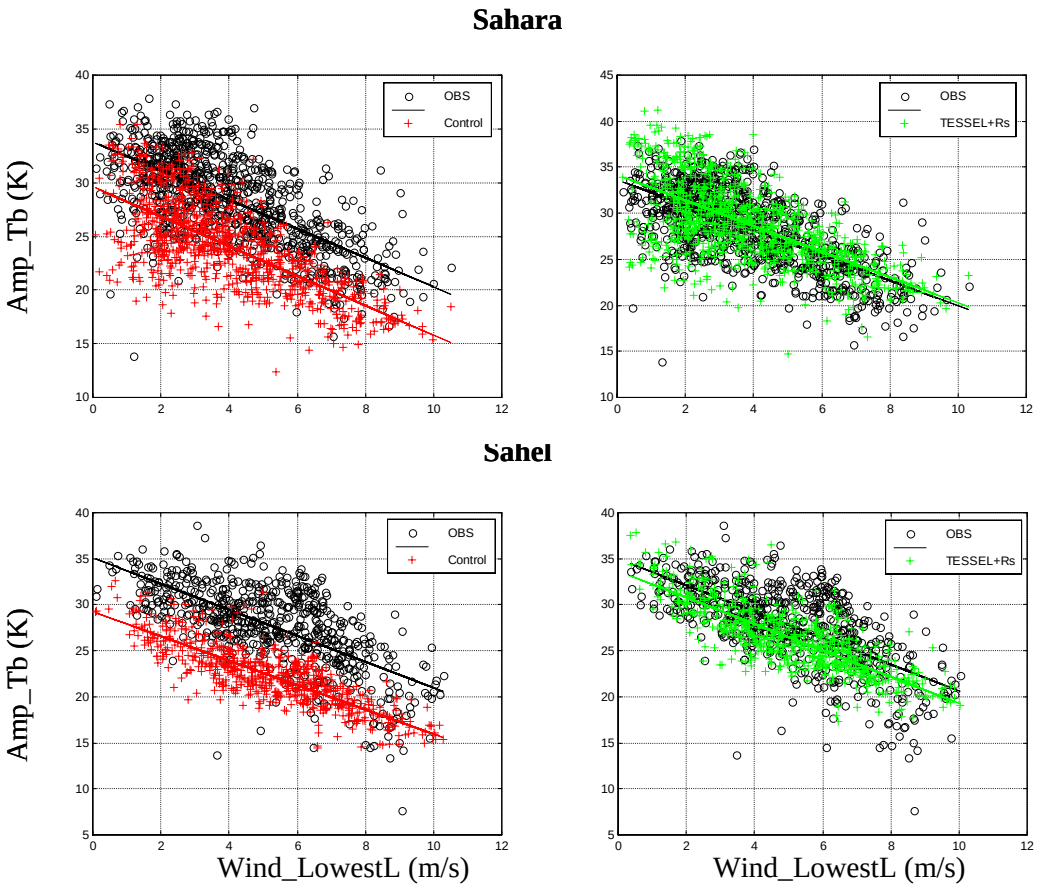

Figure 11: Amplitude of brightness temperatures (K; Tb at 12 UTC minus Tb at 3 UTC) plotted against the wind at the lowest model level (m/s), for the Sahara (top panels) and the Sahel regions (lower panels). + *– control run;* + *– modified run;* ***o*** *– Meteosat Tb observations.*

Acknowledgments

The kind help and discussions with Pedro Viterbo and Anton Beljaars are greatly appreciated. The modifications, regarding the treatment of subgrid orographic drag introduced in the ECMWF model version CY26R3 (used as control in section 4), were performed by Anton Beljaars.

References

Betts, A. K, and A. C. M. Beljaars (1993). Estimation of effective roughness length for heat and momentum from FIFE data. *Atmos. Res.*, **30**, 251-261.

Betts, A. K, J. H. Ball, A. C. M. Beljaars, M. J. Miller, and P. Viterbo, (1996). The land surface-atmosphere interaction: a review based on observational and global modelling perspectives. *J. Geophys. Res.*, **101**, 7209-7225.

Eyre, J. R., (1991). *A fast radiative transfer model for satellite sounding systems*. ECMWF Tech. Memo. No. 176, 28 pp.

Köhler, M. and J. Teixeira, (2002). *ECMWF single column model – reference and user's guide. Cycle 23r4.* 18pp., available from ECMWF, Reading, UK.

Kustas, W. P., and J. M. Norman, (2000). A two-source energy balance approach using directional radiometric temperature observations for sparse canopy covered surfaces. *Agron. J.*, **92**, 847-854.

Lutz, H.-J., (1999). *Cloud processing for Meteosat second generation.* EUMETSAT Technical Memorandum No. 4, 26 pp.

Malhi, Y., (1996). The behaviour of the roughness length for temperature over heterogeneous surfaces. *Q. J. R. Meteorol. Soc.*, **122**, 1095-1125.

Norman, J. M., W. P. Kustas, and K. K. Humes, (1995). A two-source approach for estimation soil and vegetation energy fluxes from observations of directional radiometric surface temperature. *Agric. Forest Meteor.*, **77**, 263-293.

Rabier, F., H. Järvinen, E. Klinker, J.-F. Mahfouf, and A. Simmons, (2000). The ECMWF operational implementation of four-dimensional variational assimilation. I: Experimental results with simplified physics. *Q. J. Roy. Meteor. Soc*., **126**, 1143-1170

Rhoads, J., R. Dubayah, D. Lettenmaier, G. O'Donell, and V. Lakshmi, (2001). Validation of land surface models using satellite-derived surface temperature. *J. Geophys. Res*., **106D**, 20,085-20,099.

Saunders, R., M. Matricardi, and P. Brunel, (1999). An improved fast radiative transfer model for assimilation of satellite radiance observations. *Q. J. Roy. Meteorol. Soc*., **125**, 1407-1425.

Trigo, I. F. and P. Viterbo, (2003). Clear sky window channel radiances: a comparison between observations and the ECMWF model. *J. App. Met*. ,**42**, 1463-1479.

van de Berg, L., J Schmetz, and J. Whitlock, (1995). On the calibration of the Meteosat water vapour channel. *J. Geophys. Res.*, **100D**, 21069-21076.

van den Hurk, B.J.J.M., P. Viterbo, A.C.M. Beljaars, and A.K. Betts, (2000). Offline validation of the ERA40 surface scheme. ECMWF Tech. Mem. 295, 42 pp.